Supporting Information

A luminescent nanoporous hybrid material based drug delivery system showing excellent theranostics potential for cancer

Arindam Modak,#[a] Ayan Kumar Barui,#[b] Chitta Ranjan Patra[b]* and Asim Bhaumik[a]*

[a]*Department of Materials Science, Indian Association for the Cultivation of Science, Jadavpur, Kolkata – 700 032, India,* [b]Lipid Science and Technology Division, CSIR-Indian Institute of Chemical Technology, Hyderabad, 500607, India

 # Contributed equally

*Address for correspondence. E-mail: crpatra@iict.res.in, patra.chitta@gmail.com (C. R. Patra); msab@iacs.res.in (A. Bhaumik)

Materials and Methods: Tris(propyliminomethyl)-phloroglucinol (TPIM-P) has been synthesized from the Schiff base condensation of 1,3,5-triformyl phloroglucinol and 3-aminopropyltriethoxysilane (APTES). 1,3,5-triformyl phloroglucinol was obtained through Duff formylation of phloroglucinol and hexamine.[1] All the reactions were carried out in flame dried glassware under nitrogen atmosphere. Na-distilled dry ethanol was used for synthesis. Phloroglucinol, hexamine, trifluoroacetic acid, hydrochloric acid, NaOH were obtained from Loba Chem., India. All solvents used for this purposes has taken from Merk, India and distilled and purified well prior use. APTES was obtained from Sigma Aldrich, USA.

MTT reagents were purchased from Calbiochem Merck KGaA, Darmstadt, Germany. The human breast cancer cell line (MCF-7) and lung cancer cell line (A549) were purchased from American Type Culture Collection (Manassas, VA). Dulbecco's modified eagle medium (DMEM), dulbecco's phosphate buffered saline (DPBS), fetal bovine serum (FBS) and penicillin/streptomycin were purchased from Sigma-Aldrich, USA.

Synthesis of Schiff base organosilane: APTES was used as organosilane precursor for its condensation with aromatic aldehyde moiety to obtain Schiff base organosilane. In a typical synthetic procedure, a solution of 1,3,5-triformylphloroglucinol (0.04 g, 0.19mmol) in dry ethanol (10 mL) was placed under nitrogen in a two-neck round-bottom flask equipped with a condenser and an addition funnel. A solution of APTES (0.209 g, 0.948 mmol) in dry ethanol (2 mL) was added drop-wise over 15 min. Within 5 min after initiating the addition, the reaction mixture becomes dark yellow in color, which was kept at reflux for 24 h after the complete addition of APTES. The mixture was allowed to cool to room temperature. Anhydrous Na2SO4 was added to the mixture to remove any moisture from the reaction mixture. This was followed by evaporation under reduced pressure in a rotary rotary evaporator. Removal of ethanol from the mixture leaves dark viscous yellowish gel (yield~80%), which was further characterized by ^{1}H, ^{13}C, FTIR and mass spectroscopy.

Synthesis of LNH-1: For the synthesis of nanoporous hybrid LNH-1 (Scheme 1.), 0.1 mol organosilane precursor was dissolved in aqueous ethanol (95 wt%) and stirred at room temperature for 5 min. 1 (M) NaOH was added later slowly with constant stirring to maintain pH of ca. 12.0. After the addition of base stirring was continued until the solution turned hazy. Later the mixture was kept in high pressure autoclave at 140°C for 3 days. Hydrothermal treatment helps the complete polymerization of silanol moieties and resulted in a robust hybrid cross-linked porous material. The product was filtered, thoroughly washed with water and ethanol and air dried to obtain deep orange solid powder designated as LNH-1 with a yield of ~75%.

Sample preparation for cell culture: A suspension of powdered LNH-1 (100 mg) in sterile TE (Tris-EDTA) buffer was prepared as a stock solution (10 mg/mL) after incubation for 5 sec in a sonicator bath to make a homogeneous suspension. Each time freshly prepared stock solution was used for all cell culture experiments.

Preparation of LNH-DOX: A series of LNH loaded doxorubicin (LNH-DOX) were prepared by incubating the various concentration of LNH-1 nanomaterials (1 µg/mL, 50 µg/mL, 200 µg/mL) with different amount of doxorubicin (0.5 µM and 2 µM) at room temperature for 2 h. Three different sets of LNH-DOX were prepared keeping the concentration of LNH-1 constant for each set, namely, LNH-1µg/mL-DOX (see in Figure 3b and SI-Fig.11a), LNH-50µg/mL-DOX (see in SI-Fig.10a and SI-Fig.11b) and LNH-200µg/mL-DOX (see in SI-Fig.10b and SI-Fig.11c). For LNH-1µg/mL-DOX, 1 µg/mL LNH-1 material was conjugated with 0.5 µM and 2 µM DOX (denoted as LNH-DOX 0.5 and LNH-DOX 2 respectively in Figure 3b and SI-Fig.11a). For LNH-50µg/mL-DOX, 50 µg/mL LNH-1 material was conjugated with 0.5 µM and 2 µM DOX (denoted as LNH-DOX 0.5 and LNH-DOX 2 respectively in SI-Fig.10a and SI-Fig.11b). For LNH-200 µg/mL-DOX, 200 µg/mL LNH-1 material was conjugated with 0.5 µM and 2 µM DOX (denoted as LNH-DOX 0.5 and LNH-DOX 2 respectively in SI-Fig.10b and SI-Fig.11c).

Characterization of LNH-DOX: LNH-DOX system has been characterized by several physicochemical techniques such as TGA (SI-Fig.7b), DLS (SI-Table-1), ^{13}C NMR (SI-Fig.8) etc. Comparing the ^{13}C CP MAS NMR of LNH-1(Fig.1.a) and LNH-DOX, it is clear that only C atoms in the vicinity of imine-N showed large chemical shifts. For doxorubicin loaded sample

carbon number 2 and 3 (Figure 1.a) showed chemical shifts of ca. 2.0 and 2.3 ppm, respectively. Since doxorubicin molecules has abundant of -OH groups which could have favorable H-bonding interaction of imine-N, these carbon atoms at the closer vicinity showed upfield chemical shifts. This results suggested favorable loading of doxorubicin in LNH-1 material.

Release kinetic study of DOX: In order to determine the release of DOX from LNH-DOX system release kinetics study was carried out in DPBS buffer (pH=7.4). In brief, 100 µL of LNH-DOX was incubated in 900 µL of DPBS for different time point (0 min-48 h) and then the solutions were centrifuged at 10000 rpm at 4°C for 10 min. The supernatant of different time points were collected and analysed in UV spectrophotometer.

***In vitro* stability study of LNH-1 and LNH-DOX:** *In vitro* stability study of LNH-1 and LNH-DOX was carried out in two physiological matrices DMEM (pH=7.4) and DPBS (pH=7.4) upto 14 days. Briefly, 100 µL of LNH-1 and LNH-DOX were incubated in DMEM and DPBS solutions. The stability study of those solutions were performed through UV-Vis spectroscopy.

Cell culture experimentation: CHO, MCF-7 and A549 cells were maintained in DMEM complete media supplemented with 10% fetal bovine serum (FBS) and 1% penicillin/streptomycin at 37°C humidified incubator with 5% CO_2 whereas HUVEC cells were maintained in EBM complete media under same condition. Cells after 70% confluency were plated into 96 well plate and 24 well plate for cell viability assay, cell cycle assay and fluorescence microscopy, respectively.

MTT assay: The MTT (3-(4,5-dimethylthiazol-2-yl)-2,5-diphenyl tetrazolium bromide) assay, a colorimetric assay, has been used for measuring the activity of enzymes that reduce MTT to formazan dyes, giving a purple color.[2] Inhibition of cancer cell proliferation was evaluated by MTT assay according to our published literature.[3] Briefly, 10, 000 of MCF-7 and A549 cells (counted by hemocytometer) were plated in each well of a 96-well tissue culture plate with 100 µL of complete DMEM media at 37°C for 24 h in humidified 5% CO_2 incubator. Next day, the media was then replaced with 100 µL (in each well) of fresh media and cells were incubated with LNH-1 nanoparticles or LNH-DOX at different concentrations for another 48 h. 1 mL of MTT stock solution (5 mg/mL) was diluted to 10 mL using DMEM media and 100 µL of this MTT solution was added to each well of 96 well plate by replacing the old media and allowed to incubate for 4 h. After 4 h, the media in each well was replaced by 100 µL of 1:1 DMSO-Methanol mixture (v/v) for solubilizing the purple formazan product. The plate was then kept on a shaker for homogeneous mixture. Finally, the microplate reader (Thermo Scientfic Varioskan Flash Reader) has been used to measure the absorbance of solution in each well of the plate at 570 nm. CHO cells were maintained and treated in the same way but for HUVEC, 6000 cells were plated in a 96 well plate already coated with collagen in EBM complete media at 37°C for 24 h in humidified 5% CO_2 incubator. Next day the EBM complete media was replaced with EBM starving media and after 12 h the cells were incubated with the LNH-1 material for next 24 h. After that the same procedure was followed except instead of use of DMEM, EBM starving media was used to dilute the MTT solution for HUVEC cells.

Cell cycle assay: Cell cycle analysis was performed according to a standard procedure by staining A549 cells with propidium iodide (PI). A549 cells were first treated with LNH-1 (100-

200 µg/mL) and after that the cells were washed in DPBS and fixed in 70% ethanol for 24 h. Cells were then re-hydrated, washed in DPBS, and treated with RnaseA mixture (50 µg/ml) followed by staining with PI (100 µg/mL). Similar experiments were done with untreated control cells in absence of LNH-1 nanomaterials. Quantification of DNA content was analysed with a FACScan flow cytometer.

Fluorescence microscopy: MCF-7, A549 and CHO cells were cultured at $2x10^4$ cells/mL/well in a 24-well plate for 24 h at humidified 37°C incubator with 5% CO_2 in DMEM media. After 24 h, the cells were incubated with LNH-1 nanoparticles for another 48 h. The cells were extensively washed with DPBS for 6 times to remove the LNH-1 nanomaterials from the surface of cell membrane. Finally, the fluorescence images of LNH-1, cancer cells (MCF-7 and A549) and CHO cells treated with LNH-1 nanomaterials were monitored by an Fluorescence Microscope (Olympus IX71, Olympus U-CMAD3, T2 Tokyo Japan) through excitation of 518 nm (green) and emission of 605 nm (red).

Characterization Techniques: ^1H and ^{13}C NMR experiments (liquid state) were carried out on a Bruker DPX-300 NMR spectrometer. Mass spectrometric data were acquired using the electron spray ionization (ESI) technique at 25–70 eV in a Micromass Q-tof-Micro Quadruple mass spectrophotometer. Carbon, hydrogen and nitrogen contents were analyzed using a Perkin Elmer 2400 Series II CHN analyzer. X-Ray diffraction patterns of the powder samples were obtained with a Bruker AXS D8 Advanced SWAX diffractometer using Cu Kα (λ=0.15406 nm) radiation. High resolution transmission electron microscopy images are recorded on a JEOL 2010 TEM operated at 200 kV. Nitrogen adsorption experiment was conducted at 77 K using a Beckman

Coulter, SA 3100 surface area measurement instrument. Prior to N_2 adsorption measurement samples were degassed in vacuum at 150°C for about 3h. Pore-size distributions were estimated employing NLDFT program and carbon/slit-cylindrical pore model as a reference. The ^{13}C cross-polarization magic angle spinning (CP-MAS) NMR spectrum was obtained on a Bruker Avance III 600WB 600 MHz at 150.9 MHz and a MAS frequency of 12 KHz. Thermogravimetry (TGA) and differential thermal analyses (DTA) of the samples were carried out in a TGA Instruments thermal analyzer TA-SDT Q-600. UV-visible diffuse reflectance spectra were recorded on a Shimadzu UV 2401PC with an integrating sphere attachment. $BaSO_4$ was used as background standard. FTIR spectra of these samples were recorded using a Nicolet MAGNA-FTIR 750 Spectrometer Series II. Fluorescence studies performed in a sealed tube by using Horiba Job in Yvon Fluoromax 3 instrument at excitation wavelengths 360 nm and 465 nm.

SI-Fig.1: Wide angle Powder XRD:

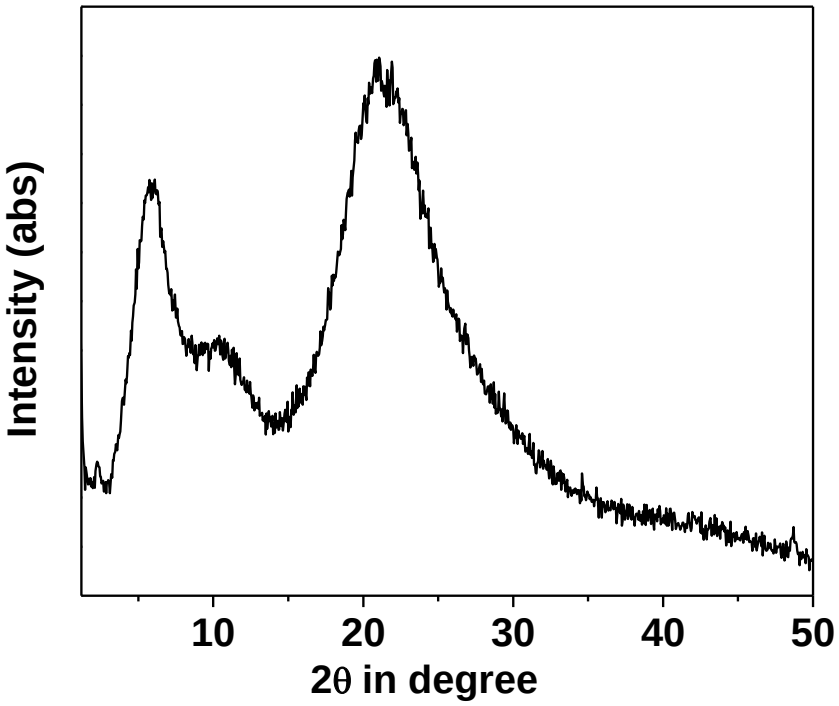

SI-Fig.1: Powder XRD pattern of hybrid nanoporous material LNH-1.

Powder X-ray diffraction pattern of LNH-1 is shown in SI-Fig.1. This pattern showed three very broad peaks centered at 5.9, 10.6 and 22.5 degrees of 2θ.

SI-Fig.2: **High magnification TEM image of LNH-1 material**

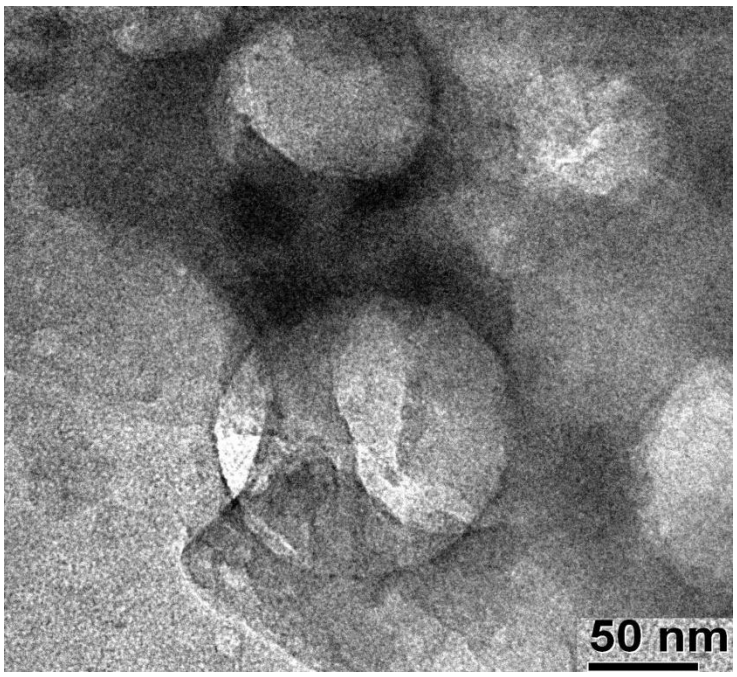

SI-Fig.2: TEM image of LNH-1 material. This is a High magnification image of the marked part of the TEM image of LNH-1 material (Fig.1d).

SI-Fig.3: Infrared spectroscopy of LNH-1 material:

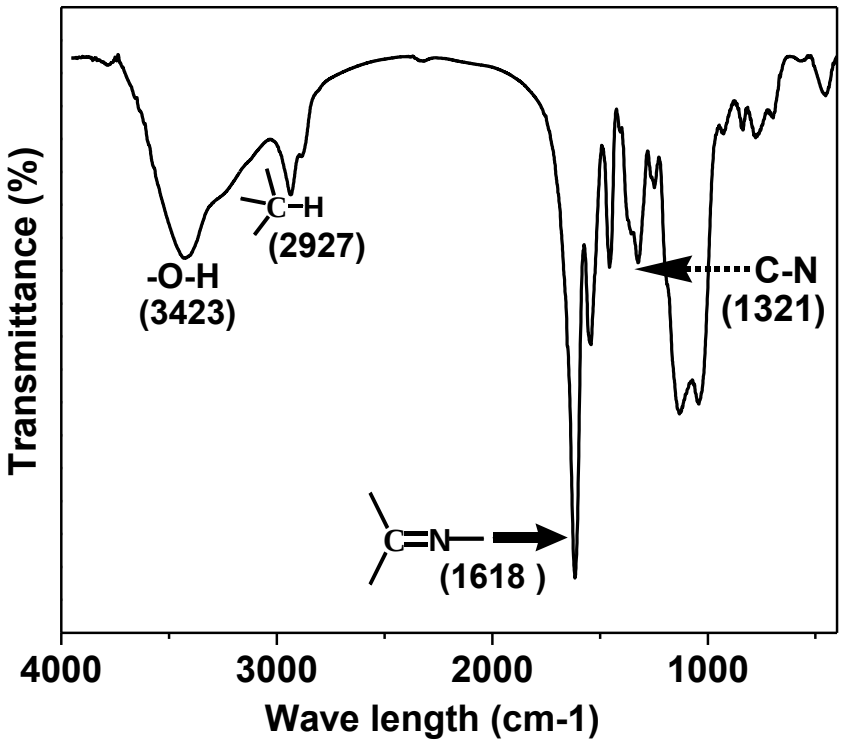

SI-Fig.3: FT-IR spectrum of organic-inorganic hybrid LNH-1 material bearing tris(propylimino methyl)-phloroglucinol fluorescent moiety in the framework.

FTIR spectra of LNH-1 exhibits several peaks in the region 3423 cm^{-1} (ν O–H, due to the presence of phloroglucinol and surface silanol groups), 2927 cm^{-1} (ν C–H), 1618, ~1512 and 1452 cm^{-1} (skeletal vibrations). In addition to C-H vibration, C-N vibration corresponding to 1321 cm^{-1} is observed. A sharp peak at 1618 cm^{-1} suggested the formation of Schiff base in the LNH-1 framework.

SI-Fig.4: **UV-Vis spectroscopy:**

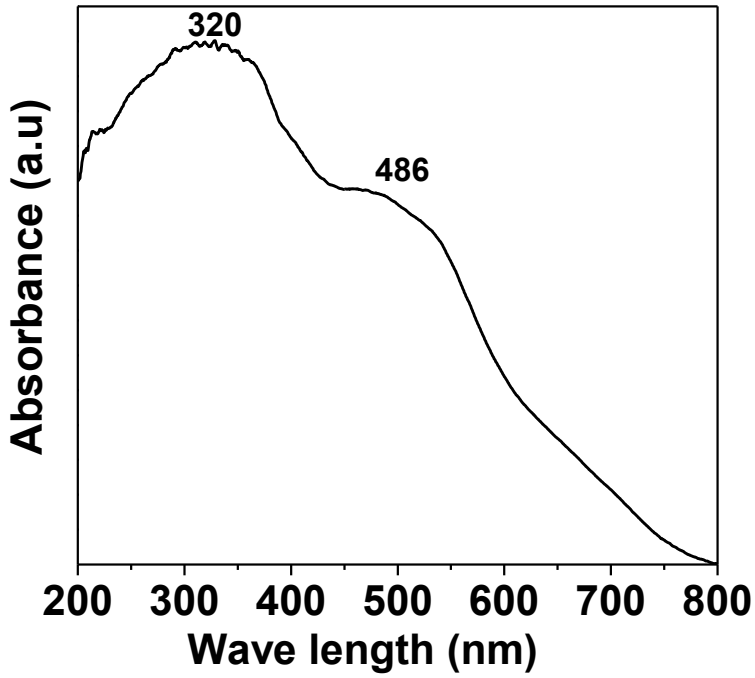

SI-Fig.4: UV–visible diffuse reflectance spectrum of LNH-1.

The UV-visible diffuse reflectance spectrum indicates characteristic strong optical absorbance of tris(propyliminomethyl)-phloroglucinol moiety in the framework. Two strong bands at 320 nm and 486 nm originates due to π→π* transitions of phenolic –OH and imine moieties.

SI-Fig.5: Nitrogen Sorption Analysis:

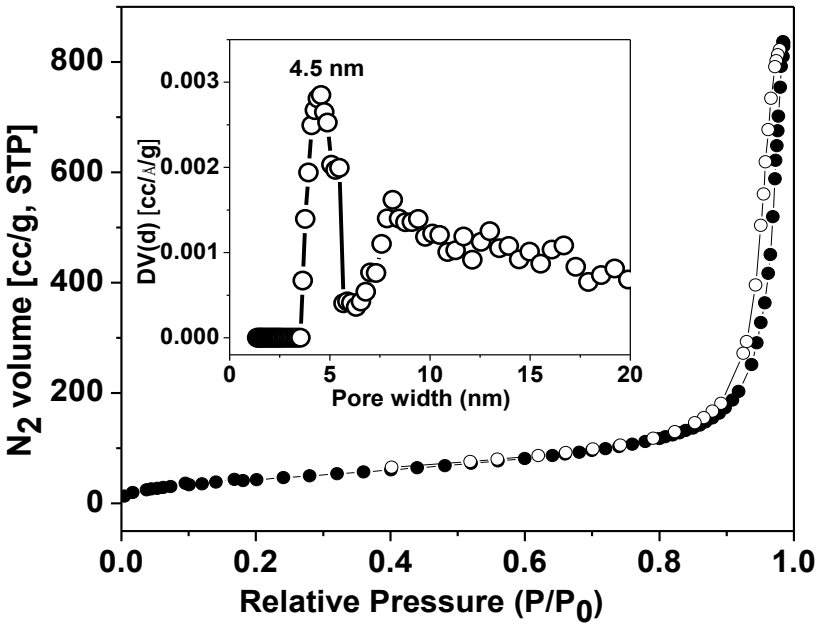

SI-Fig.5: N_2 adsorption/desorption isotherms and pore size distribution of LNH-1 at 77 K. Pore size distribution estimated through NLDFT equilibrium method has been shown in the inset of the figure.

Porosity of this nanomaterial has been estimated from N_2 adsorption desorption isotherm and the corresponding Brunauer-Emmett-Teller (BET) surface area was found to be 175 m^2g^{-1}. The isotherm exhibits flat extrapolation from the low pressure region and substantial entanglement at very high pressure with low hysteresis during desorption which indicates that in addition to the presence of micropores, intermolecular mesoporosity also present significantly in LNH-1 material. Pore size distribution (shown in the inset of the SI-Fig.5) has been carried out using NLDFT equilibrium mode (cylindrical pore, N_2 at 77K on carbon). Pore volume and average pore diameter was found to be 0.899 ccg^{-1} and 4.5 nm respectively.

SI-Fig.6: Biocomaptibility of LNH-1 in MCF-7 cells

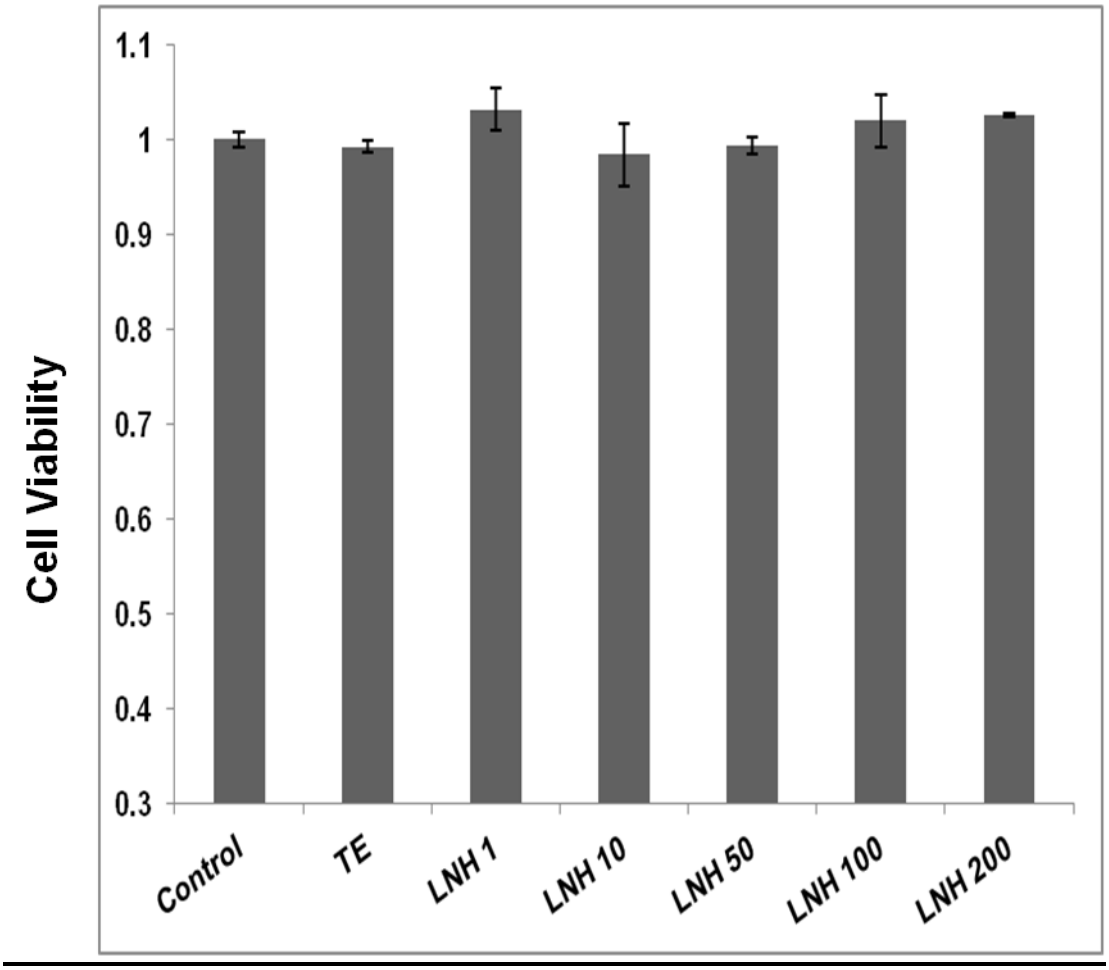

SI-Fig.6: Biocomaptibility of LNH-1 in MCF-7 cells using MTT assay. Cell viability of MCF-7 cells using LNH-1 nanomaterials was demonstrated by MTT assay in a dose dependent fashion (1-200 µg/mL). The results show that MCF-7 cells are viable upto 200 µg/mL. Tris EDTA (TE) buffer was used as vehicle control experiment.

SI-Fig. 7 (a-b): TGA patterns of LNH-1 and LNH-DOX:

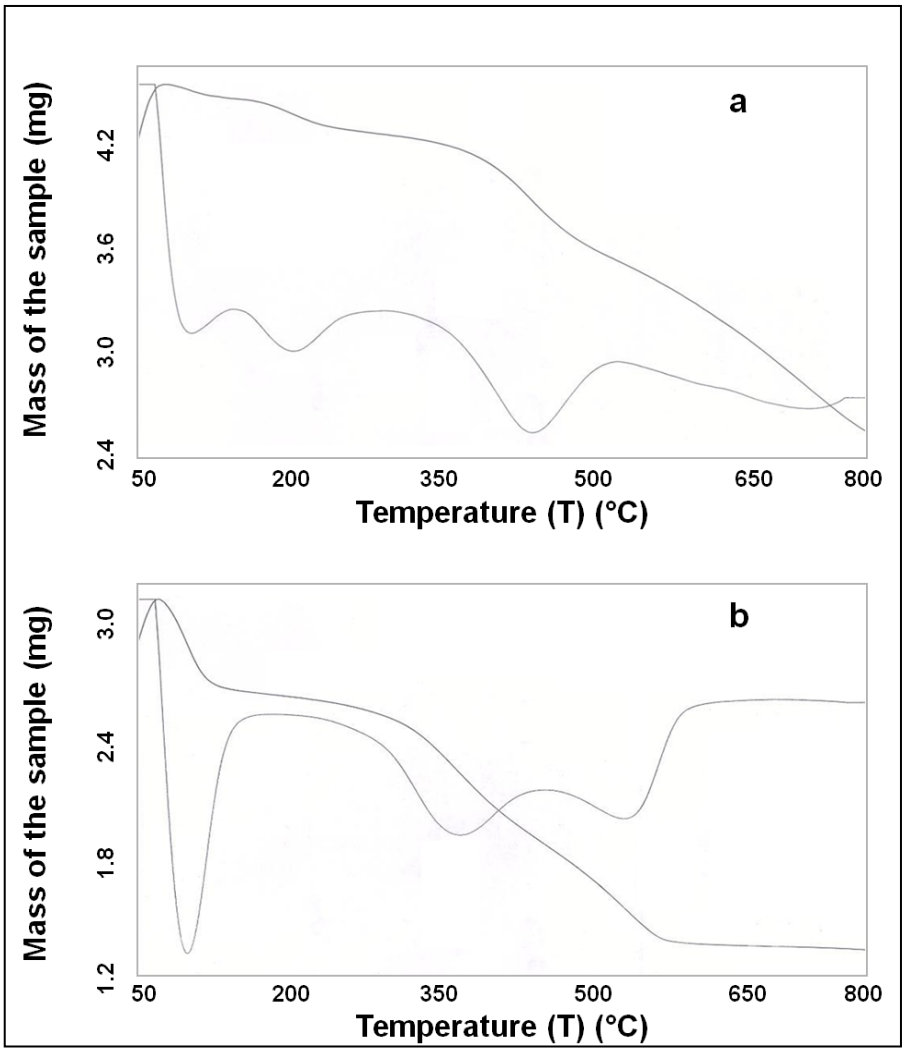

SI-Fig.7 (a-b): TGA analysis of LNH-1 and LNH-DOX. (a) For LNH-1 total weight loss is 44.83% and (b) For LNH-DOX total weight loss is 61.56%. The endothermic peaks in both pictures correspond to the derivative curve of the TGA profiles of LNH-1 and LNH-DOX system.

To determine the binding efficiency of DOX with LNH-1 in LNH-DOX system the TGA profiles of LNH-1 and LNH-DOX materials have been checked. SI-Fig. 7a and 7b represent the TGA patterns of LNH-1 and LNH-DOX respectively. In this SI-Fig.7 the endothermic curves indicate the corresponding derivative curve of the TGA patterns. In both cases for LNH-1 and LNH-DOX three weight losses have been appeared. For LNH-1, the first and the second weight loss occurs at 60°C-130°C and 140°C-170°C corresponding to the 1.75% and 4.39% of the total weight loss which may be due to the loss of residual water molecules present on the surface of LNH-1. The third weight loss happens at 320°C-800°C with 38.02% of the total weight loss which may be due to the loss of organic fragments present in LNH-1. These three weight losses are also indicated by the derivative curve which shows endothermic peak at temperature 80°C, 180°C and 440°C. The total weight loss for LNH-1 is about 44.83%. For LNH-DOX, there are weight losses at the temperature range 60°C -130°C (12.61% of total weight loss), 250°C-440°C (18.01% of total weight loss) and 450°C-600°C (15.91% of total weight loss) due to the loss of residual water, loss of DOX molecules attached with LNH-1 and lastly the loss of organic fragments of the LNH-1. These three losses are indicated by the endothermic peak in the derivative curve at 80°C, 350°C and 550°C. The total weight loss of LNH-DOX system is about 61.56%. From these TGA patterns of LNH-1 and LNH-DOX it is calculated that the % of binding of DOX in LNH-DOX system is 5.9%. It can be also calculated from this % of binding of DOX that there may be 1.4×10^{15} number of DOX molecules loaded per mg of LNH-DOX DDS.

Table-1: DLS study of LNH-1, DOX and LNH-DOX:

Sample	***Zeta (mV)***
LNH-1	***5.1***
DOX	***12.5***
LNH-DOX	***16.9***

Table 1: DLS study. The zeta potential values of LNH-1, DOX and LNH-DOX have been known from the DLS study. Here all the zeta values are positive and indicates the absence of any electrostatic interaction present between LNH-1 and DOX to form the LNH-DOX system.

SI-Fig. 8: ^{13}C CP MAS NMR of LNH-DOX material:

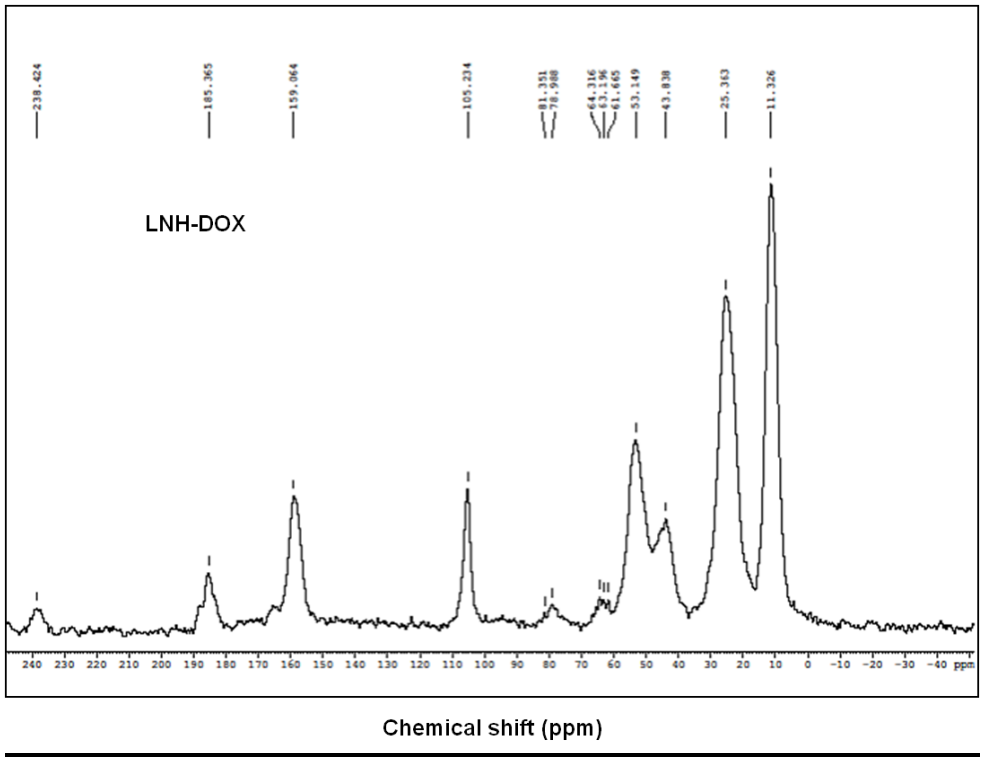

SI-Fig.8: ^{13}C CP MAS NMR of LNH-DOX material. Comparing the ^{13}C CP MAS NMR of LNH-1(Fig.1.a) and LNH-DOX, it is clear that only C atoms in the vicinity of imine-N showed large chemical shifts. For doxorubicin loaded sample carbon number 2 and 3 (Figure 1.a) showed chemical shifts of ca. 2.0 and 2.3 ppm, respectively. Since doxorubicin molecules has abundant of -OH groups which could have favorable H-bonding interaction of imine-N, these carbon atoms at the closer vicinity showed upfield chemical shifts. This results suggested favorable loading of doxorubicin in LNH-1 material.

SI-Fig. 9: In vitro stability study of LNH-1 and LNH-DOX:

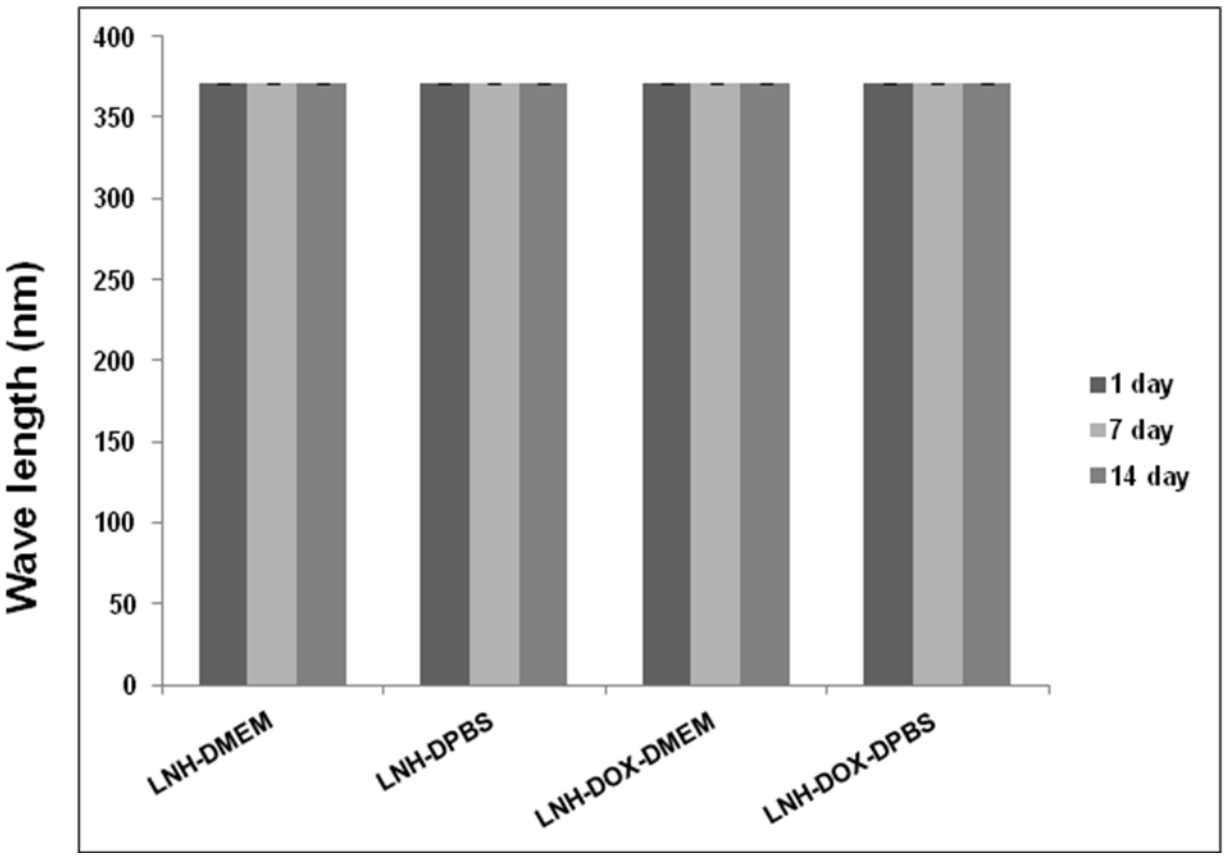

SI-Fig.9: *In vitro* stability studies of LNH-1 and LNH-DOX materials. This study shows the high stability of all the materials in two biological matrices DMEM and DPBS (1 day-14 day) as the wave length of the materials do not vary with the elapse of time in different physiological solutions.

SI-Fig.10 (a-b): Cell viability of LNH-DOX (LNH: 50 µg/mL and 200 µg/mL) in A549 cells:

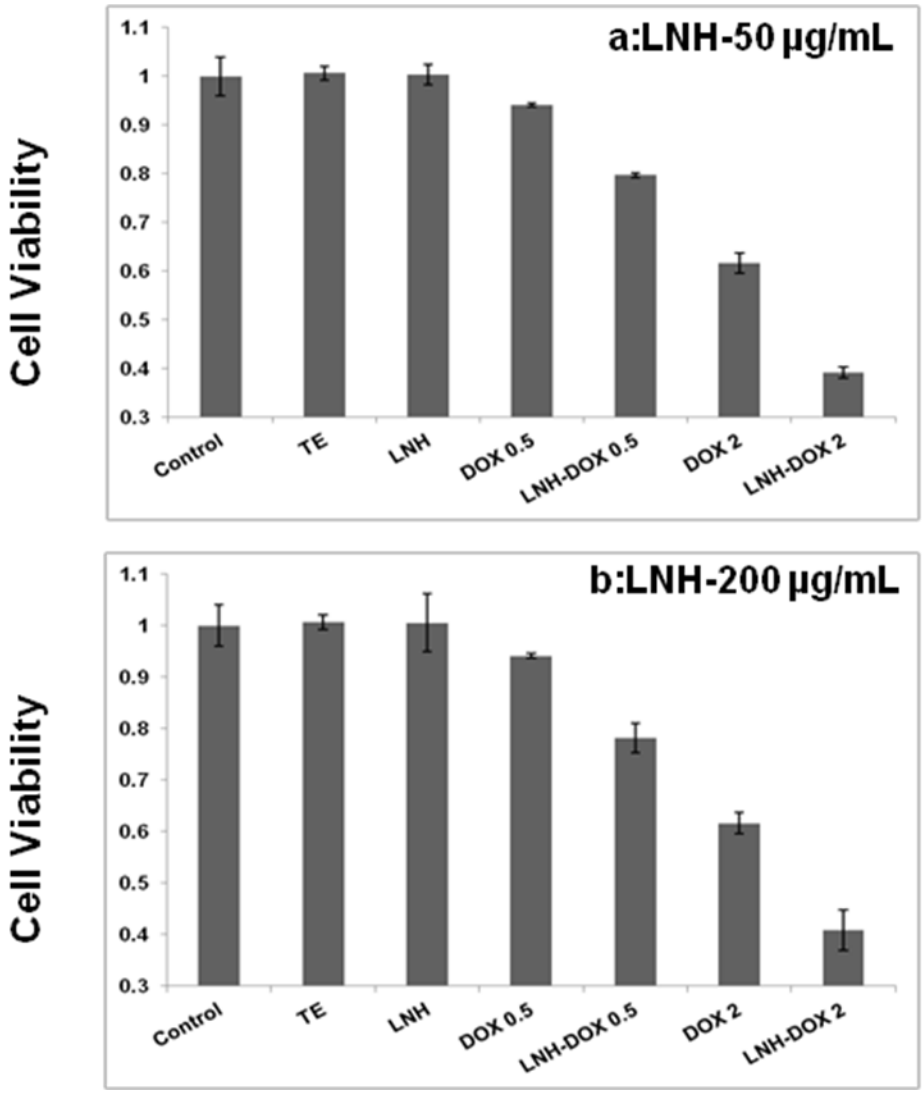

SI-Fig.10 (a-b): Application of LNH-1 as delivery vehicle in MCF-7 cells using MTT assay. Doxorubicin loaded LNH-1 nanomaterials show higher therapeutic efficacy in a dose dependent manner compared to control free doxorubicin. (a) A549 cells were incubated with 50 µg of LNH-1 nanomaterials. (b) A549 cells were incubated with 200 µg of LNH-1 nanomaterials. DOX 0.5 and DOX 2 indicate the 0.5 µM and 2 µM concentrations of doxorubicin respectively.

SI-Fig.11 (a-c): Cell viability of LNH-DOX (LNH: 1 µg/mL, 50 µg/mL and 200 µg/mL) in MCF-7 cells:

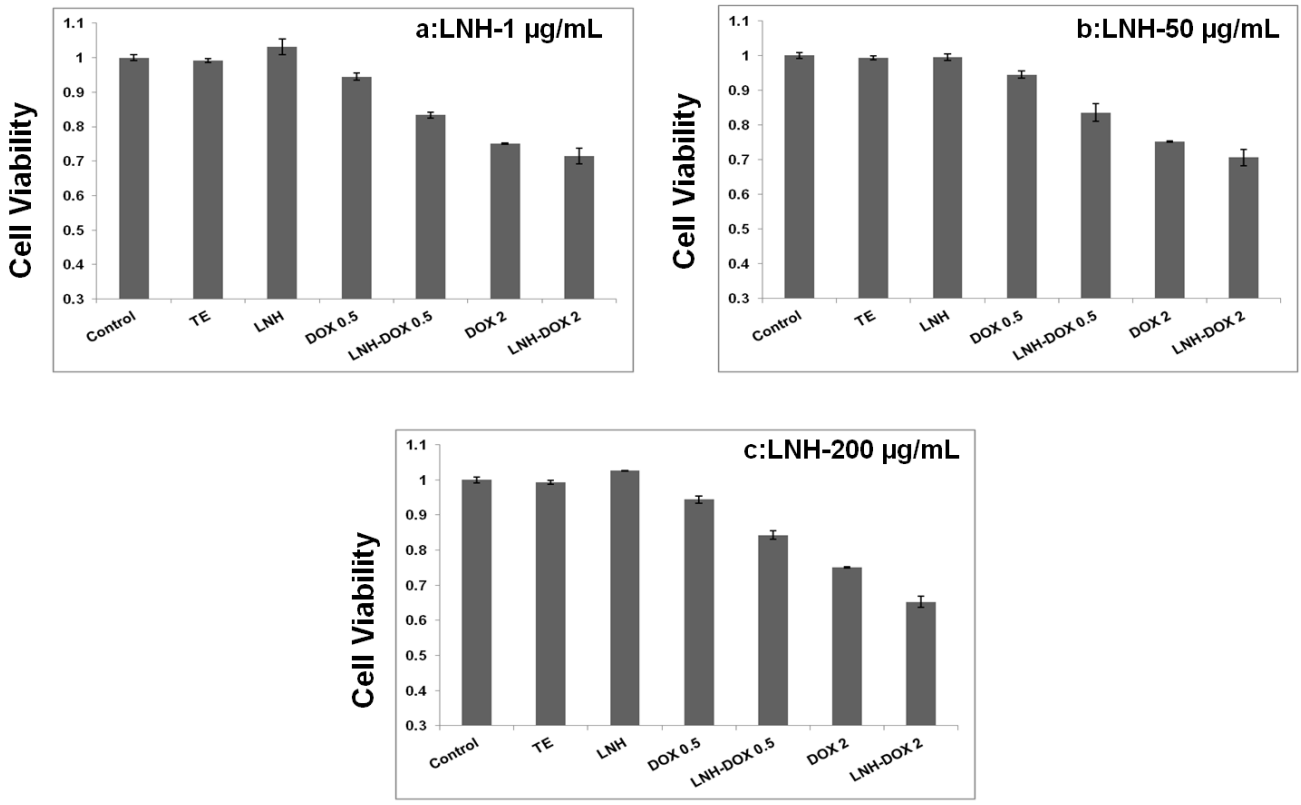

SI-Fig.11 (a-c): Application of LNH-1 as delivery vehicle in MCF-7 cells using MTT assay. Doxorubicin loaded LNH-1 nanomaterials show higher therapeutic efficacy in a dose dependent manner compared to control free doxorubicin. (a) A549 cells were incubated with 1 µg of LNH-1 nanomaterials. (b) A549 cells were incubated with 50 µg of LNH-1 nanomaterials and (c) A549 cells were incubated with 200 µg of LNH-1 nanomaterials. DOX 0.5 and DOX 2 indicate the 0.5 µM and 2 µM concentrations of doxorubicin respectively.

SI-Fig.12: Fluorescence imaging studies in MCF-7 cells in different plates:

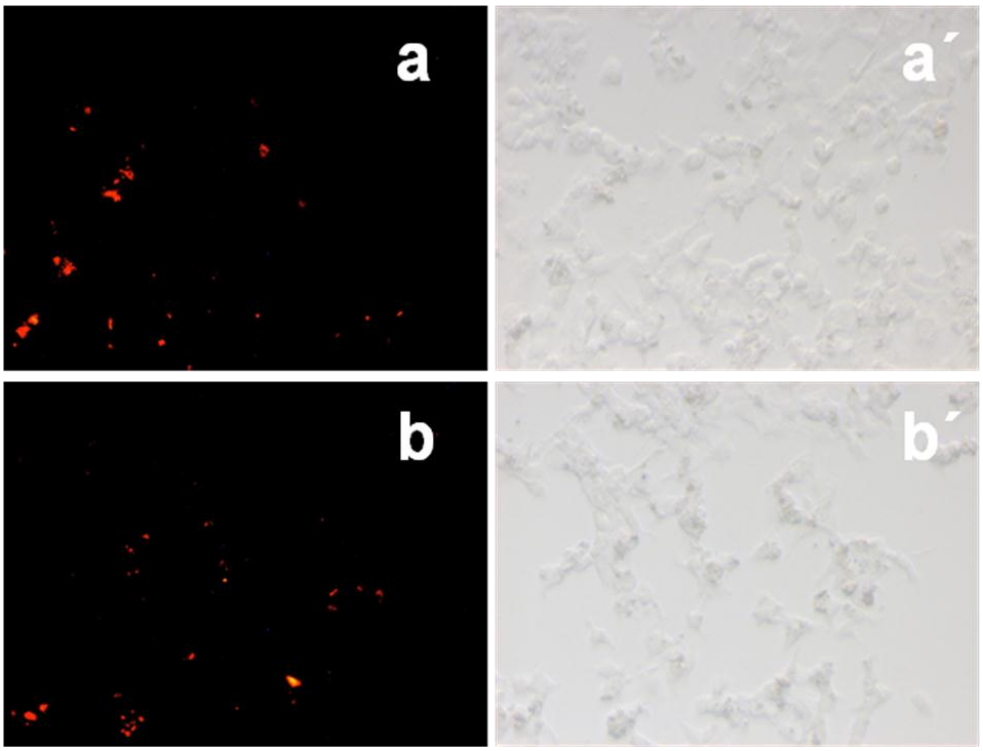

SI-Fig.12 (a-a´; b-b´): Fluorescence (a-b) and its corresponding phase images (a´-b´) of MCF-7 cells treated with LNH-1 nanoparticles at different wells of 24 plates (as we have done the experiment in triplicate), observed by Olympus Fluorescence Microscope. The LNH-1 nanoparticles treated MCF-7 cells were extensively washed with DPBS (6 times) before taking the fluorescence images.

SI-Fig.13: Fluorescence imaging studies in A549 cells:

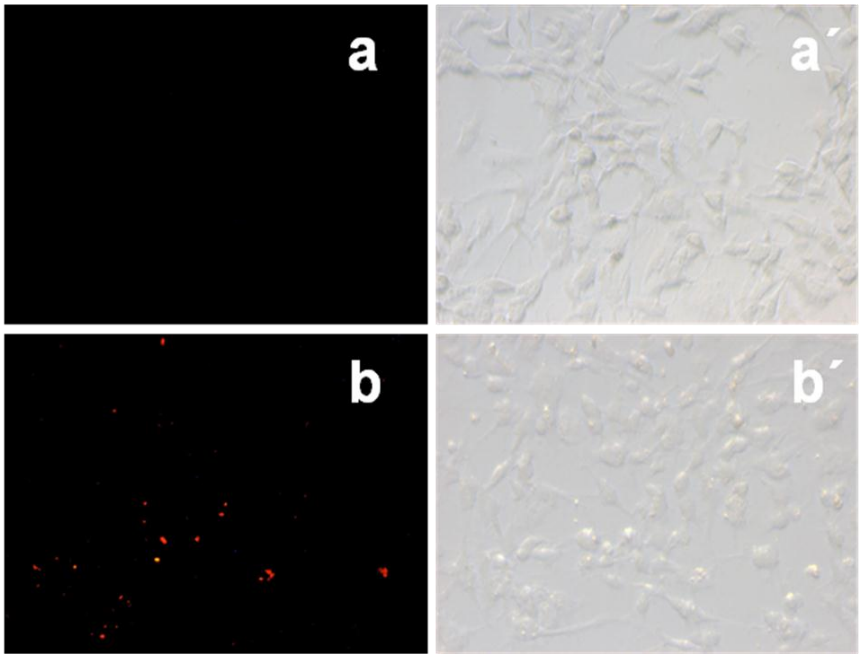

SI-Fig.13 (a-a´; b-b´): Fluorescence (a-b) and its corresponding phase images (a´-b´) of A549 cells, observed by Olympus Fluorescence Microscope. (a-a´): fluorescence image of untreated A549 cells and its corresponding phase image. (b-b´): fluorescence image of A549 cells treated with LNH-1 nanoparticles and its corresponding phase image. The LNH-1 nanoparticles treated A549 cells were extensively washed with DPBS (6 times) before taking the fluorescence images.

SI-Fig.14: Fluorescence imaging studies in CHO cells:

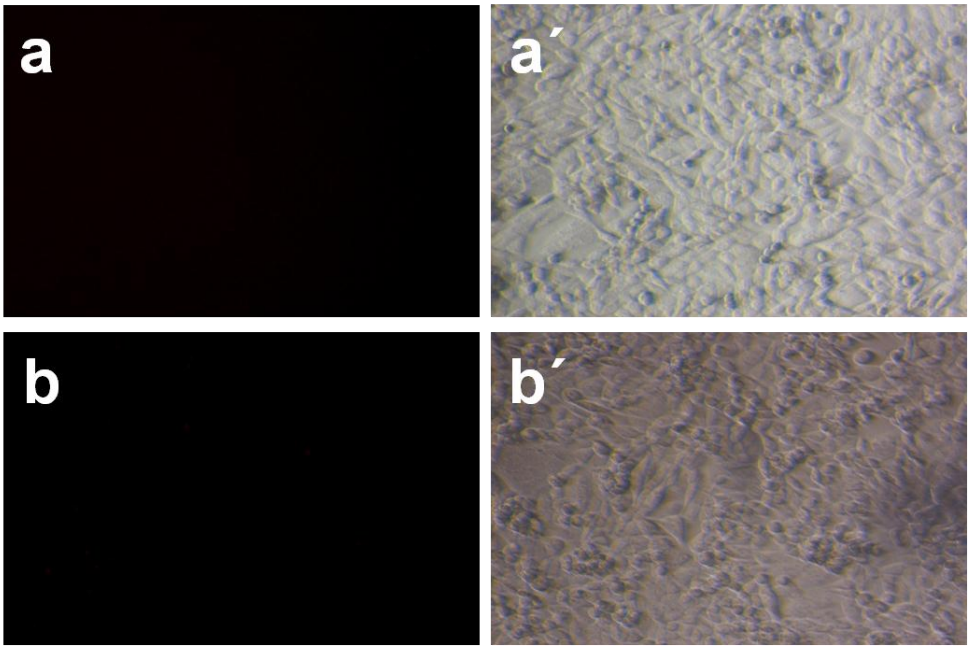

SI-Fig.14 (a-a´; b-b´): Fluorescence (a-b) and its corresponding phase images (a´-b´) of CHO cells, observed by Olympus Fluorescence Microscope. (a-a´): fluorescence image of untreated CHO cells and its corresponding phase image. (b-b´): fluorescence image of CHO cells treated with LNH-1 nanoparticles and its corresponding phase image. The LNH-1 nanoparticles treated CHO cells were extensively washed with DPBS (6 times) before taking the fluorescence images.

^{1}H and ^{13}C NMR chemical shifts, FTIR and MS data of tris(propyliminomethyl-triethoxysilyl)-phloroglucinol organosilane precursor:

^{1}H NMR (500 MHz, $CDCl_3$) δ = 0.68 (t, J=4.5Hz, 6H), 1.30 (t, J=7Hz, 27H), 1.54 (m, 6H), 3.51 (t, J= 7 Hz, 6H), 3.79 (q, J= 7Hz, 18H), 8.19 (m, 3H), 11.3 (s, broad, 3H) ppm. ^{13}C NMR (125 MHz, $CDCl_3$) δ = 8.9, 23, 20, 52, 58, 104, 158, 166 ppm. HRMS calculated for $C_{36}H_{69}N_3Si_3O_{12}$: [M+]: 820.512. Found: 820.5130; [M++H]: 821.5148. FTIR (KBr): ν = 2977, 1609, 1552, 1446, 1316, 1072, 950, 738 cm^{-1}.

References:

1	C. V. Yelamaggad, A. S. Achalkumar, D. S. S. Rao and S. K. Prasad, *J. Org. Chem.*, 2009, **74**, 3168.
2	L. Wang, J. S. Lau, C. R. Patra, Y. Cao, S. Bhattacharya, S. Dutta, D. Nandy, E. Wang, C. N. Rupasinghe, P. Vohra, M. R. Speller and D. Mukhopadhyay, *Molecular Cancer Research*, 2010, **8**, 1591; (b) T. J. Mosmann, *Immunol. Methods*, 1983, **65**, 55.
3	N. T. Patil, P. G. V. V. Lakshmi, B. Sridhar, S. Patra, M. Pal Bhadra, C. R. Patra, *Eur. J. Org. Chem.*, 2012, **9**, 1790.